

## A ketogenic diet increases transport and oxidation of ketone bodies in RG2 and 9L gliomas without affecting tumor growth

Henk M. De Feyter, Kevin L. Behar, Jyotsna U. Rao, Kirby Madden-Hennessey, Kevan L. Ip, Fahmeed Hyder, Lester R. Drewes, Jean-François Geschwind, Robin A. de Graaf, and Douglas L. Rothman

Department of Radiology and Biomedical Imaging, Magnetic Resonance Research Center, Yale University School of Medicine, New Haven, Connecticut (H.M.D.F., J.U.R., K.M.-H., K.L.I., J.-F.G., R.A.D., D.L.R.); Department of Psychiatry, Magnetic Resonance Research Center, Yale University School of Medicine, New Haven, Connecticut (K.L.B.); Department of Biomedical Sciences, University of Minnesota, Duluth, Minnesota (L.R.D.); Department of Biomedical Engineering, Yale University, New Haven, Connecticut (F.H., R.A.D., D.L.R.)

**Corresponding Author:** Henk M. De Feyter, PhD, Yale University School of Medicine, Department of Radiology and Biomedical Imaging, 300 Cedar Street, P.O. Box 208043, New Haven, CT 06520-8043 (henk.defeyter@yale.edu).

See the editorial by Rieger and Steinbach, on pages 1035–1036.

**Background.** The dependence of tumor cells, particularly those originating in the brain, on glucose is the target of the ketogenic diet, which creates a plasma nutrient profile similar to fasting: increased levels of ketone bodies and reduced plasma glucose concentrations. The use of ketogenic diets has been of particular interest for therapy in brain tumors, which reportedly lack the ability to oxidize ketone bodies and therefore would be starved during ketosis. Because studies assessing the tumors' ability to oxidize ketone bodies are lacking, we investigated *in vivo* the extent of ketone body oxidation in 2 rodent glioma models.

**Methods.** Ketone body oxidation was studied using  $^{13}\text{C}$  MR spectroscopy in combination with infusion of a  $^{13}\text{C}$ -labeled ketone body (beta-hydroxybutyrate) in RG2 and 9L glioma models. The level of ketone body oxidation was compared with nontumorous cortical brain tissue.

**Results.** The level of  $^{13}\text{C}$ -beta-hydroxybutyrate oxidation in 2 rat glioma models was similar to that of contralateral brain. In addition, when glioma-bearing animals were fed a ketogenic diet, the ketone body monocarboxylate transporter was upregulated, facilitating uptake and oxidation of ketone bodies in the gliomas.

**Conclusions.** These results demonstrate that rat gliomas can oxidize ketone bodies and indicate upregulation of ketone body transport when fed a ketogenic diet. Our findings contradict the hypothesis that brain tumors are metabolically inflexible and show the need for additional research on the use of ketogenic diets as therapy targeting brain tumor metabolism.

**Keywords:**  $^{13}\text{C}$  MRS, glioma, ketogenic diet, MCT1, metabolism.

A ketogenic diet (KD)—high fat, adequate protein, minimal carbohydrate—leads to increased levels of ketone bodies in plasma while reducing the glucose concentration, creating a nutrient profile similar to that of long-term fasting. Such a nutritional condition could be energetically challenging for tissues that heavily rely on glucose for their energy metabolism, such as the brain. However, neurons (and glial cells) can replace a substantial part of their oxidative energy (ATP) production from glucose by oxidation of ketone bodies.<sup>1,2</sup> Brain tumors, on the other hand, are believed to lack the enzymes to oxidize ketone bodies.<sup>3–6</sup> High-grade brain tumor energy metabolism presumably relies heavily on the Warburg effect: a high rate of glucose metabolism through glycolysis accompanied by lactic acid production in the presence of ample oxygen. The Warburg effect is often explained as caused by dysfunctional

mitochondria. The idea of dysfunctional mitochondria and the supposed lack of ketolytic enzymes have led to the conclusion that brain tumors have limited ability to oxidize ketone bodies.<sup>5,7</sup> With reduced capacity to produce ATP from ketone body oxidation, a KD could result in a glucose-dependent brain tumor being starved. This “metabolic inflexibility” of brain tumors has led to promoting KDs as alternative or adjunct treatment for standard brain tumor therapies.<sup>4–12</sup>

The interest in applying KDs as part of brain tumor management is evident from feasibility studies and clinical trials that are currently recruiting participants<sup>13–15</sup> (clinicaltrials.gov). Data in support of the cancer-inhibiting effect of a KD in humans are limited to case reports.<sup>16–18</sup> Several, but not all, studies of animal models of various cancer types have shown positive effects of KDs on tumor growth and survival, either as

Received 17 June 2015; accepted 28 March 2016

© The Author(s) 2016. Published by Oxford University Press on behalf of the Society for Neuro-Oncology. All rights reserved.

For permissions, please e-mail: journals.permissions@oup.com.

single treatment or in combination with other therapies.<sup>6,10,19–25</sup> Evidence of impaired ketone body oxidation in tumors is mostly based on *in vitro* data, and acquired under nutritional conditions different from when fed a KD.<sup>3,6,11,26,27</sup> Furthermore, recent metabolic data of tissue excised from patients infused with <sup>13</sup>C-labeled glucose and acetate have clearly shown oxidative metabolism in brain tumors.<sup>28,29</sup> Therefore, *in vivo* data on brain tumor ketone body metabolism when fed a standard diet and under KD conditions are warranted to validate the mechanism of a KD as nutritional therapy targeting brain tumor metabolism.

We applied <sup>13</sup>C magnetic resonance spectroscopy (MRS), a method that uniquely allows the study of metabolic pathways *in vivo*, in combination with infusion of <sup>13</sup>C-labeled *D*-beta-hydroxybutyrate (BHB), the ketone body with the highest plasma level during (diet-induced) ketosis. We used *in vivo* <sup>1</sup>H-[<sup>13</sup>C] MRS to measure the fractional <sup>13</sup>C enrichment of glutamate as proof of [2,4-<sup>13</sup>C<sub>2</sub>]-BHB oxidation in 2 rat glioma cell lines, 9L and RG2, after orthotopic implantation (Fig. 1).<sup>30</sup> The 9L model, a gliosarcoma model, is the most commonly studied rat brain tumor model, while RG2 shows histopathological features resembling human glioblastoma.<sup>31</sup> *In vivo* BHB transport and metabolism in the gliomas were compared with the contralateral, nontumorous brain. The effect of a calorie-restricted KD on tumor growth was also investigated. In accordance with the current paradigm, we hypothesized that both tumor models would show substantially reduced oxidative ketone metabolism during infusion of [2,4-<sup>13</sup>C<sub>2</sub>]-BHB compared with nontumorous brain tissue, reflected by low levels of glutamate <sup>13</sup>C-labeling (Fig. 1). We also hypothesized that analogous to mouse brain tumor models, tumor growth would be slower when fed a KD and animals would live longer.<sup>4,6,8,10,25,32</sup>

## Materials and Methods

### Cell Lines

The 9L and RG2 cells were purchased from American Type Culture Collection (ATCC) and not further tested or authenticated.

Working stocks were created from cells at an early passage (between 4 and 7) by freezing in medium with dimethyl sulfoxide as cryopreservant and stored in liquid nitrogen. No cells were used beyond 30 passages. Cells were grown in 75 cm<sup>2</sup> flasks at 37°C in humidified air and 5% CO<sub>2</sub> in Dulbecco's modified Eagle's medium (DMEM; Gibco), supplemented with 10% heat-inactivated fetal bovine serum (Gibco) and 1% penicillin-streptomycin (Gibco).

### Orthotopic Xenograft Tumor Model

Male Fischer rats (F344/DuCrI, Charles River Laboratories) were anesthetized with isoflurane using O<sub>2</sub> as carrier gas via a nosecone and fitted in a stereotactic rodent frame (David Kopf Instruments). After shaving and antiseptic treatment, an incision was made along the midline of the scalp. A burr hole was made using a drill (0.6 mm bit) 3 mm to the right of bregma and 1 mm anterior to the coronal suture. The amount of tumor cells (ATCC) injected was 10<sup>5</sup> and 1250 for the 9L and RG2 tumor models, respectively, suspended in 5 μL serum-free DMEM. A 25 μL Hamilton syringe with 25 gauge needle was inserted 3 mm below the cortical surface by lowering 3.5 mm and retracting 0.5 mm. The burr hole was covered with bone wax (Ethicon) and the incision closed with 3.0 suture thread (Monocryl Plus Antibacterial, Ethicon). All animal procedures were approved by the Yale University Institutional Animal Care and Use Committee.

### Ketogenic Diet

Animals were randomly put on a KD (91% fat and 9% protein, Harlan Teklad #TD96355) 1 week after tumor cell inoculation. The diet was provided in the animals' cage daily in a calorie-restricted way. The amount of KD was increased in case body weight was reduced >20% from baseline. The composition of the standard diet (Harlan Teklad #2018) was 23% protein, 17% fat, and 60% carbohydrates.

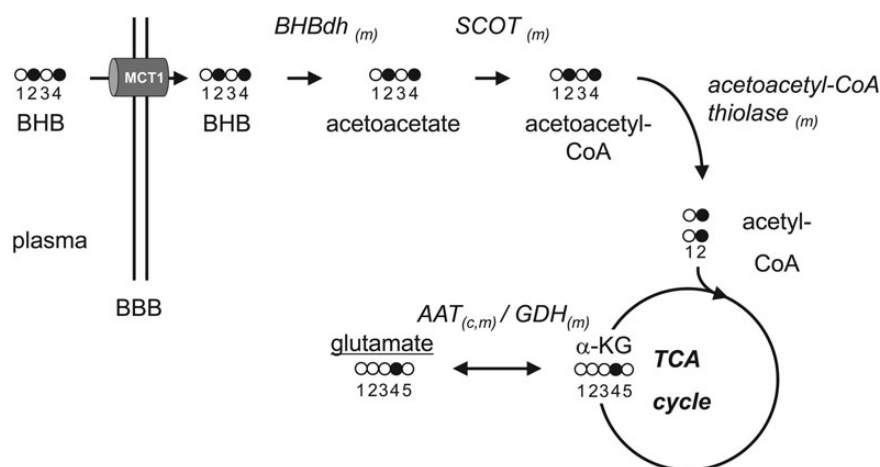


**Fig. 1.** Oxidative metabolism of ketone bodies. Schematic overview of [2,4-<sup>13</sup>C<sub>2</sub>]-BHB metabolism in brain showing <sup>13</sup>C-labeling of glutamate C4 (for first turn of the TCA cycle). Filled circles represent <sup>13</sup>C, open circles represent <sup>12</sup>C. BHBdh, BHB dehydrogenase; SCOT, succinyl-CoA acetoacetyl-CoA transferase; Co-A, co-enzyme A; α-KG, α-ketoglutarate; (m), mitochondrial; (c) cytosolic; TCA, tricarboxylic acid; AAT, aspartate amino transferase; GDH, glutamate dehydrogenase; BBB, blood-brain barrier.

## MRI/MR Spectroscopy

In vivo nuclear MR measurements were performed using a 9.4T horizontal bore magnet interfaced to an Agilent spectrometer. MR images were acquired between 9 and 25 days post-inoculation using a quadrature  $^1\text{H}$  radiofrequency surface coil after intravenous injection of 200  $\mu\text{L}$  of the  $T_1$  contrast agent gadopentetate dimeglumine (Magnevist, Bayer). In animals used for MRS, a femoral vein and artery were catheterized for infusion of  $[2,4\text{-}^{13}\text{C}_2]$ -BHB and blood sampling, respectively. A combined quadrature  $^{13}\text{C}$  and single loop  $^1\text{H}$  surface coil setup was used to acquire MR spectra from voxels (32–90  $\mu\text{L}$ ) positioned in tumor and contralateral, nontumorous brain (Fig. 2A and B). A proton-observed carbon-edited (POCE) sequence with laser localization was used with repetition time/echo time of 2.5 s/25(17 + 8) ms (Fig. 2D–F).<sup>30</sup> MRS acquisition started together with infusion of  $[2,4\text{-}^{13}\text{C}_2]$ -BHB and continued for 96 min. At the end of the infusion and MRS acquisition, animals were quickly removed from the MR scanner and euthanized using focused-beam microwave irradiation.<sup>33</sup> The brain was removed and tumor and tissue samples of nontumorous cortex dissected and stored at  $-80^\circ\text{C}$  until extract preparation. All extracts and plasma analyses were performed in mixtures containing phosphate buffer (100 mM),  $\text{D}_2\text{O}$  (60  $\mu\text{L}$ ), Na-formate (2 mM) as chemical shift reference, and imidazole (2 mM) using a 500 MHz MR spectrometer (Bruker Avance).

## Histology

Histochemical analysis was performed on 4- $\mu\text{m}$ -thick sections of perfusion-fixed tissue (4% paraformaldehyde) embedded in

paraffin. Immunostaining was performed as previously described.<sup>34</sup> In short, staining procedures included hematoxylin and eosin (H&E) for determining brain and glioma structure. Other stains performed were glial fibrillary acidic protein (GFAP) to visualize reactive gliosis, and Ki-67 as marker for proliferation. An antibody against CD68 was used to identify cells with a macrophage background. Staining for the monocarboxylic transporter 1 (MCT1) was performed on RG2 tumors from animals fed the standard diet and the KD, respectively. Details on antibody source, dilutions, and incubation times are described in the Supplementary material.

## Statistics

Statistical analysis was performed using SPSS 21 (IBM). Group differences were investigated using dependent and independent  $t$ -tests. Survival was analyzed using the log-rank test. Statistical significance was set at  $P = .05$ . All data are presented as mean  $\pm$  SD.

## Results

### In vitro BHB Metabolism in 9L and RG2 Cells in High-Glucose Medium

Both 9L and RG2 cell lines were cultured in high-glucose medium (25 mM) and switched to relatively low glucose medium (5.6 mM) with 4 mM  $[2,4\text{-}^{13}\text{C}_2]$ -BHB for 6 h. Glucose and BHB consumption and lactate production were calculated from media samples, and data are shown in Supplementary Fig. S1. In RG2 cells there was evidence of low BHB uptake

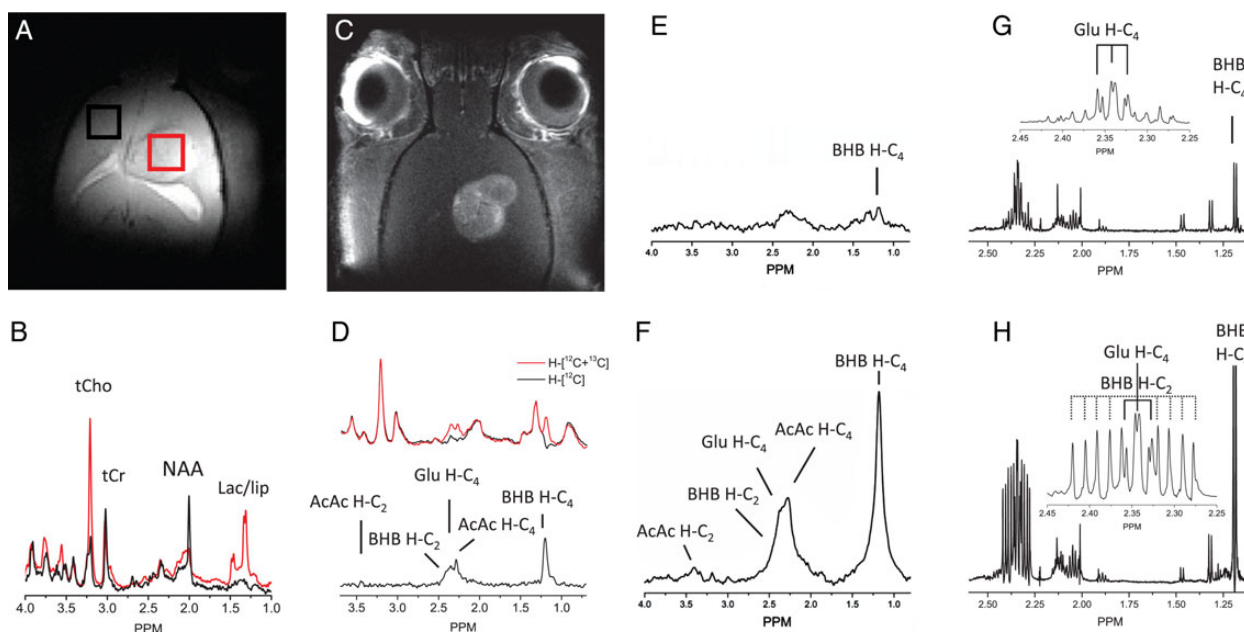


**Fig. 2.** MRI and MRS in glioma-bearing rats. (A) Coronal gradient-echo MRI of 9L-bearing rat with MRS voxels located in tumor and contralateral brain. (B)  $^1\text{H}$  MR spectra acquired in brain (black) and tumor (red) from voxels depicted in (A). (C)  $T_1$ -weighted coronal spin-echo MRI after i.v. injection of gadolinium contrast agent in RG2-bearing rat. (D) Example of POCE spectra from 9L following  $[2,4\text{-}^{13}\text{C}_2]$ -BHB infusion. Top spectra originate from  $^1\text{H}$  attached to  $^{12}\text{C}$  and  $^{13}\text{C}$  (black), and  $^1\text{H}$  attached to  $^{12}\text{C}$  only (red). The difference spectrum (below) reveals signal from  $^{13}\text{C}$ -bound  $^1\text{H}$  only. In vivo (E and F) and tissue extract (G and H)  $^1\text{H}$ - $[^{13}\text{C}]$  MR difference spectra acquired from RG2 glioma tissue from rats fed the standard diet (E and G) and a KD (F and H) after 96 min of  $[2,4\text{-}^{13}\text{C}_2]$ -BHB infusion. Insets: zoom of spectral region of glutamate H-C<sub>4</sub> and BHB H-C<sub>2</sub>. PPM, parts per million; peak annotations; tCho, total choline; tCr, total creatine; NAA, N-acetylaspartate; Lac, lactate; lip, lipid; AcAc, acetoacetate; BHB,  $\beta$ -hydroxybutyrate; Glu, glutamate.

and BHB oxidation, indicated by  $^{13}\text{C}$ -labeling of glutamate C4 in cell extracts ( $^{13}\text{C}$  fractional enrichment:  $7.9\% \pm 0.5\%$ ). RG2 cells therefore had sufficient mitochondrial enzyme capacity to oxidize ketone bodies in vitro. Similar results were reported by Eloqayli et al in C6 rat glioma cells.<sup>35</sup> In 9L cells, uptake of BHB was not detectable, and no substantial  $^{13}\text{C}$  fractional enrichment was detected above the 1.1% natural abundance level ( $1.9\% \pm 0.9\%$ ). These data accordingly identify 9L cells as lacking observable capacity to oxidize BHB in vitro.

### Rat Glioma Models 9L and RG2

Orthotopic implantation of 9L and RG2 cells resulted in the expected development of brain tumors, which could be observed on MRI (Fig. 2).  $^1\text{H}$  MR spectra acquired from tumors show features typically observed in human gliomas: increased choline/creatinine and reduced levels of N-acetyl aspartate (NAA) compared with normal brain (Fig. 2B). Examples of immunohistochemical staining of rat brains with 9L and RG2 gliomas are shown in Fig. 3. The staining revealed the well-described appearance of 9L and RG2 tumors with high cell density (H&E), high degree of proliferation (Ki-67), and signs of reactive gliosis

at the border of the tumors (GFAP). No immunoreactivity was observed with the marker for macrophage lineage cells (CD68), indicating negligible infiltration of immune cells. Successful staining of macrophages in rat spleen (Fig. 3P) assured that lack of positive CD68 staining in glioma tissue was not a false-negative result.

### In vivo $[2,4-^{13}\text{C}_2]$ -BHB Metabolism in 9L and RG2 Gliomas

Plasma levels of glucose and BHB were significantly different between standard diet and KD conditions and confirmed the intended plasma nutrient profile of low glucose and high BHB when fed the KD to metabolically challenge the gliomas (Fig. 4A).

Infusion of  $[2,4-^{13}\text{C}_2]$ -BHB increased blood plasma levels of both BHB and acetoacetate in all rats, while  $^{13}\text{C}$  label incorporation into glucose  $\text{C}_1$  by systemic metabolism was low ( $<3\%$ ) and similar for both tumor types (Supplementary Table S1). Upon infusion of  $^{13}\text{C}$ -BHB in 9L- and RG2-bearing rats fed the standard diet, tissue BHB levels tended to be higher in gliomas compared with cortical tissue (Fig. 4B), yet the level of variability prevented reaching statistical significance ( $0.05 < P < .07$ ).

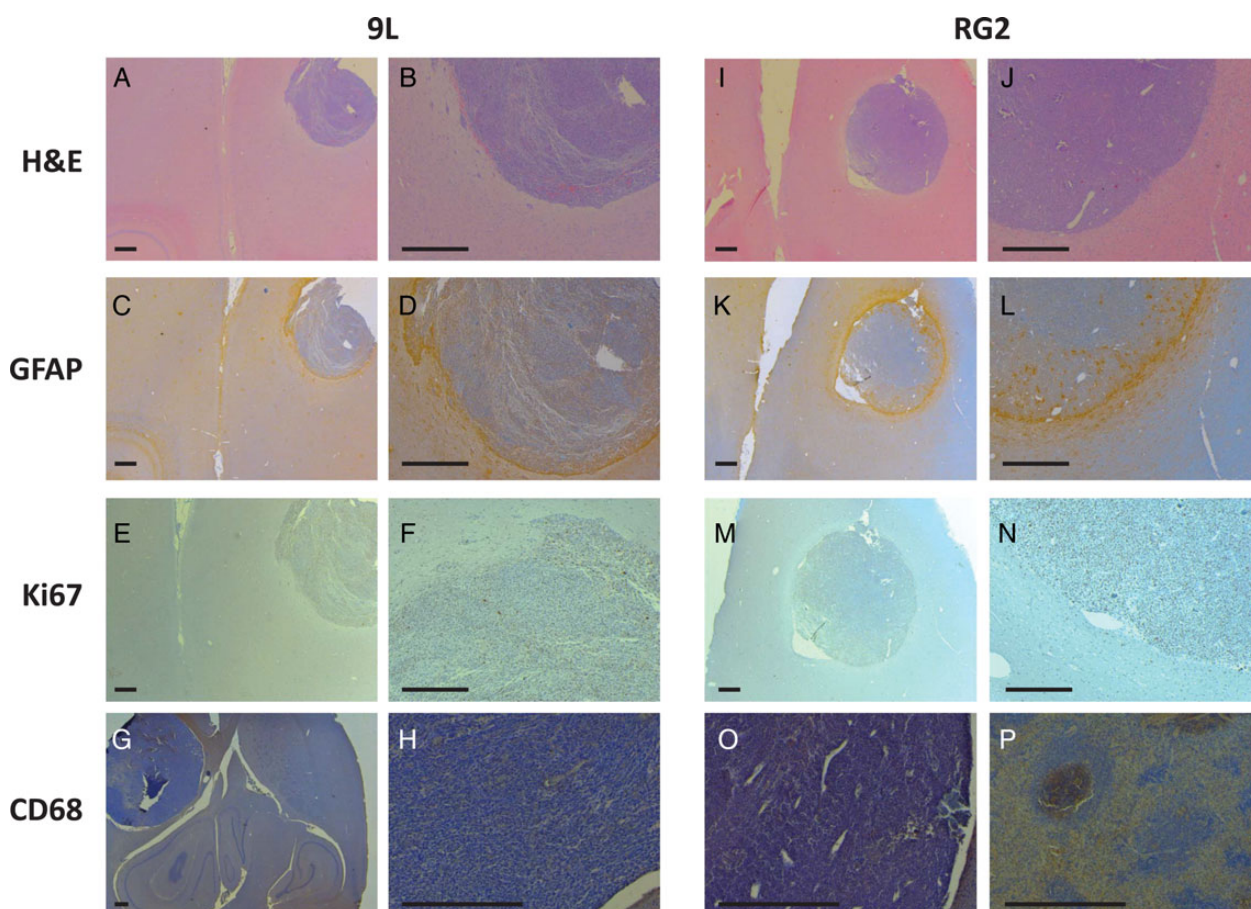


**Fig. 3.** Immunohistochemistry. (A–H) Staining results from rat brains containing 9L and (I–O) RG2 gliomas. Hematoxylin (blue, cell nuclei) and eosin (pink, cytoplasm) staining on top row shows gliomas embedded in brain tissue. Other stains included hematoxylin to indicate cell nuclei in addition to diaminobenzidine (brown) for visualizing antibodies targeting reactive gliosis (GFAP, C, D, K, L), cell proliferation (Ki-67, E, F, M, N), and macrophages (CD68, G, H, O, P). The bottom row shows staining results for macrophages in gliomas (G, H, O) and spleen (P). Note the very low immunoreactivity for CD68 (brown) in brain and tumor tissue, but high signal in spleen tissue (P). Scale bar represents 100  $\mu\text{m}$ .

Tissue BHB concentration increased following feeding the KD in both 9L and RG2 gliomas and cortex. The KD-induced BHB increase was more pronounced in gliomas, resulting in significantly higher BHB levels in gliomas compared with normal brain (Fig. 4B).

Glutamate fractional  $^{13}\text{C}$  enrichment, the indicator of  $^{13}\text{C}$ -BHB oxidation, was substantial (15%–20%) and similar (or slightly higher) in 9L and RG2 gliomas compared with normal cortex when fed the standard diet (Fig. 4C). In a pattern similar to the increase of tissue BHB, glutamate fractional enrichment doubled in both cortex and gliomas after animals were fed the KD (Fig. 4C). Estimates of BHB oxidation from the steady state metabolic model indicate the similar relative levels of BHB oxidation ( $V_{\text{BHB}}/V_{\text{TCA}}$ ) in cortex and gliomas and confirmed the increase in BHB oxidation in both tissues following the KD intervention (Supplementary Table S2).

### MCT1 Immunohistochemistry

To clarify the increased BHB tumor levels in the KD condition, we investigated the level of MCT1. MCT1 allows passive bidirectional transport of monocarboxylic acids (ie, lactate, pyruvate, acetate, and BHB). Stronger MCT1 immunoreactivity was observed in RG2 glioma tissue of animals fed the KD (Fig 5A and

B; MCT1-positive pixels, standard diet vs KD:  $14.5\% \pm 3.5\%$  vs  $30.9\% \pm 12.9\%$ ,  $P = .057$ ).

### Effect of KD-Mimicking Cell Culture Conditions, and Explanted 9L Cells

The prominent feature of a KD is the lowered glucose and increased levels of ketone bodies in plasma. Standard cell culture media contain very high levels of glucose (25 mM) and little to no ketone bodies compared with the in vivo condition. We therefore tested the hypothesis that relatively low glucose and high BHB levels in the cell culture medium could induce BHB uptake and metabolism and explain the discrepancies between the in vitro and in vivo results. Tumor cells were first grown in low glucose conditions (5.6 mM), and later BHB (4 mM) was added to the medium. After 3–4 passages, no increase in BHB uptake or metabolism was observed in either low glucose or low glucose with BHB compared with high glucose (25 mM) growth conditions (Supplementary Fig. S1).

To further investigate the differences in metabolism between in vitro and in vivo cell growth, we explanted a 9L tumor and created a cell line (9L-expl). We challenged all the cell lines (9L, RG2, and 9L-expl) to very low glucose conditions (2.5 mM) and added 8 mM BHB. In none of the cell lines did the

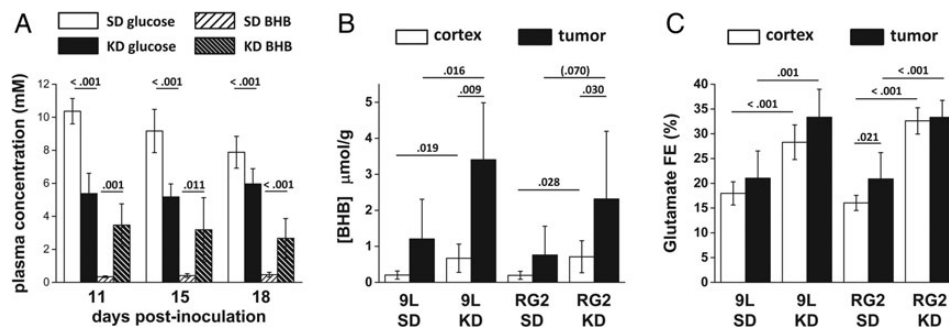


**Fig. 4.** Plasma nutrients and BHB uptake and metabolism. (A) Plasma concentration of glucose and BHB measured in venous blood at 11, 15, and 18 days post-inoculation of glioma cells. SD, standard diet, KD, ketogenic diet. SD after 11 and 15 days:  $n = 7$ , after 18 days:  $n = 17$ ; KD after 11 and 15 days:  $n = 8$ , after 18 days:  $n = 18$ . (B) BHB concentration in cortex (open bars) and tumor tissue (black bars) of 9L and RG2-bearing rats fed SD or ketogenic KD measured at the end of the 96 min  $[2,4-^{13}\text{C}_2]$ -BHB infusion. (C) Glutamate  $^{13}\text{C}$  fractional enrichment (FE; %) in cortex and tumor tissue of 9L and RG2-bearing rats fed SD and KD measured at the end of the 96 min  $[2,4-^{13}\text{C}_2]$ -BHB infusion. (B and C) Group sizes  $n = 7$ . Data presented as mean  $\pm$  standard deviation and relevant  $P$ -values indicated.

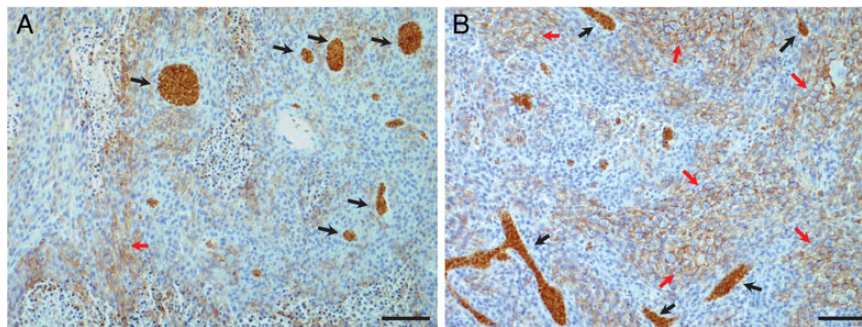


**Fig. 5.** Immunohistochemistry of MCT1. Immunohistological staining of MCT1 (brown) and cell nuclei (light blue) in RG2 glioma tissue of rats fed (A) the standard diet and (B) the ketogenic diet. Black arrows indicate nonspecific staining of red blood cells in vessels/hemorrhagic lesions in the tumors. Red arrows point to prominent immunoreactivity in cell membranes. Notice the increased MCT1 immunoreactivity in RG2 glioma tissue of a rat fed the ketogenic diet (B). Bar represents 100  $\mu\text{m}$ .

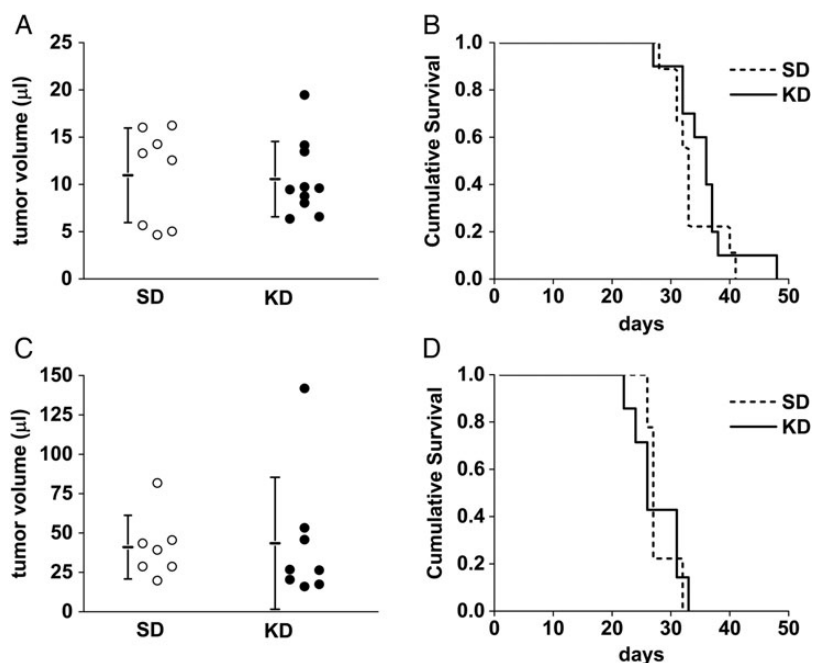


**Fig. 6.** Tumor volume and survival. (A) MRI-based tumor volume 21 days post-inoculation and (B) Kaplan–Meier survival analysis for 9L-bearing rats (9L SD:  $n = 11$ , 9L KD:  $n = 10$ ,  $P = .42$ ). (C) MRI-based tumor volume 18 days post-inoculation and (D) Kaplan–Meier survival analysis for RG2-bearing rats (RG2 SD:  $n = 9$ , RG2 KD:  $n = 10$ ,  $P = .48$ ). SD, standard diet, KD, ketogenic diet. Data presented as mean  $\pm$  standard deviation.

addition of BHB rescue reduced cell growth induced by 2.5 mM glucose levels (Supplementary Fig. S2).

### Effect of KD on Plasma, Body Weight, and RG2 Glioma Growth

We evaluated the anticancer effect of the KD in both 9L- and RG2-bearing rats. For the KD to be effective in targeting the proposed metabolic inflexibility of brain tumors, high BHB and low glucose levels in plasma need to be established. In rodents, this can require feeding a KD in a calorie-restricted way. Yet, a calorie-restricted diet can result in significant loss of body weight. To reduce the potentially confounding effect of severe weight loss, we adjusted the amount of KD provided to the animals day-to-day based on the measured body weight. Feeding the KD this way resulted in lowered glucose levels and increased BHB concentrations in plasma (Fig. 3A); however, body weight was also significantly affected (Supplementary Fig. S4). Despite fulfilling the conditions for a KD to be successful, there was no effect on MRI-based tumor volume measured 21 (9L) or 18 days (RG2) after tumor cell inoculation, nor was a survival benefit observed in animals fed the KD (Fig. 6). Similarly, the cumulative survival for both glioma models (Fig. 6) did not show a positive effect of the KD (log-rank analysis; 9L:  $P = .415$ ; RG2:  $P = .476$ ).

## Discussion

There is a growing interest to use KDs as metabolic therapy for (brain) tumors. The main proposed mechanism for a KD-induced metabolic anticancer effect relies on the ideas

that (brain) tumor cells have a high obligatory need for glucose, are metabolically relatively inflexible, and have limited capacity to oxidize ketone bodies. By lowering glucose and elevating ketone bodies through a KD, such tumors could effectively be starved of energy. A limitation of previous work on KDs as brain tumor therapy has been the absence of *in vivo* metabolic studies. Here we investigated ketone body metabolism in 2 rat glioma models using  $^1\text{H}$ - $^{13}\text{C}$  MRS and the  $^{13}\text{C}$ -labeled ketone body [2,4- $^{13}\text{C}_2$ ]-BHB.

As depicted in Fig. 1, oxidative metabolism of [2,4- $^{13}\text{C}_2$ ]-BHB requires BHB dehydrogenase (BHBdh, EC1.1.1.30), succinyl-CoA acetoacetyl-CoA transferase (SCOT, EC2.8.3.5), and acetoacetyl-CoA thiolase (EC2.3.1.9) to produce two [2- $^{13}\text{C}$ ]-acetyl-CoA molecules; [2- $^{13}\text{C}$ ]-acetyl-CoA can then enter the tricarboxylic acid cycle, labeling the intermediate metabolites, which through fast exchange with  $\alpha$ -ketoglutarate leads to  $^{13}\text{C}$ -labeling of glutamate. In the present study  $^{13}\text{C}$ -labeling of glutamate was therefore the primary outcome parameter *in vitro* and *in vivo* to determine the presence of ketone body oxidation in RG2 and 9L cells.

Our main findings were the *in vivo* evidence of ketone body oxidation in both 9L and RG2 glioma models at similar levels as normal brain tissue and the adaptive nature of MCT1 expression that facilitated ketone body transport and metabolism. We hypothesized that oxidative metabolism of BHB would be significantly reduced in the 9L and RG2 rat gliomas. However, during infusion of [2,4- $^{13}\text{C}_2$ ]-BHB in both 9L and RG2 gliomas  $^{13}\text{C}$ -labeling of glutamate was detected *in vivo* (Figs 2 and 4). Therefore, the premise that brain tumors have limited enzyme capacity to oxidize ketone bodies does not apply to these tumor models when studied *in vivo*. Steady state metabolic modeling confirmed that ketone bodies contributed approximately 20%

of oxidative metabolism in both 9L and RG2 tumors when animals were fed a standard diet, which increased to 35%–40% when fed the KD, similar to normal brain (Supplementary Table S2). In other words, the tumor cells and neural cells oxidized the same amount of BHB relative to all of the substrates available (primarily glucose, lactate, glutamine). Therefore, the premise that brain tumors have limited enzyme capacity to oxidize ketone bodies does not apply to the 9L and RG2 tumor models when studied *in vivo*.

The *in vivo* and *ex vivo* MRS methods used in this study do not have the spatial resolution to allow discriminating different cell types that could contribute to the observed  $^{13}\text{C}$ -BHB oxidation. A first indication that the tumor volumes selected for *in vivo* MRS do not contain a fraction of neuronal cells sufficient to explain the labeling results is the lack of the neuronal marker NAA in the  $^1\text{H}$  MR spectra, analogous to  $^1\text{H}$  MR spectra acquired in glioma patients (Fig. 2B). Histological evaluation using multiple stains of rat brains containing 9L and RG2 gliomas (Fig. 3) indicates that tumor cells make up the vast majority of the tissue. Glioma tissue also contained minimal amounts of reactive glial cells and invading immune cells. The histological staining results therefore confirm that glioma cells are responsible for the vast majority of  $^{13}\text{C}$ -BHB oxidation detected in tumors using  $^1\text{H}$ - $^{13}\text{C}$  MRS.

The capacity of tumor cells to oxidize ketone bodies has so far been investigated by evaluating enzymes of the ketolysis pathway using extraction methods, mRNA detection, enzyme protein levels in animal models and cell lines,<sup>3,6,26</sup> and histology in human glioma tissue.<sup>27</sup> The expression levels of ketolytic enzymes were reported to be mostly lower compared with control tissue, and these data led to justify a KD as a metabolic therapy to starve brain tumors.<sup>3,6,11,26,27</sup> Notably, none of the previous studies have investigated ketone body metabolism in tumors *in vivo* and *after* being exposed to a KD. The differences found here between the *in vivo* and *in vitro* metabolism of ketone bodies underscore the relevance of studying tumors in their actual microenvironment.

Our MRS data not only showed clear evidence of oxidative ketone body metabolism in the rat gliomas but also revealed an adaptation induced by the KD that promoted uptake of BHB from the blood. BHB transport across the blood–brain barrier of normal brain occurs along the BHB concentration gradient via MCT1, which facilitates proton-linked transport of monocarboxylates.<sup>36</sup> An increase in the plasma–tissue concentration gradient could therefore explain the higher tissue BHB levels following the  $[2,4\text{-}^{13}\text{C}_2]$ -BHB infusion in KD-fed animals. Infusion of  $[2,4\text{-}^{13}\text{C}_2]$ -BHB adds to the existing blood-borne BHB, which is higher in animals fed the KD. However, in both 9L and RG2 KD-fed animals, higher levels of plasma BHB compared with animals fed the standard diet (1.2 times higher for 9L and 2.5 times higher for RG2; Supplementary Table S1) following infusion of  $[2,4\text{-}^{13}\text{C}_2]$ -BHB cannot completely account for the increased tissue BHB levels in 9L gliomas (2.8 times higher) or RG2 gliomas (3 times higher). Therefore, another mechanism besides an increased BHB concentration gradient must add to higher BHB levels observed following a KD. Feeding rats a KD has been shown to induce an increase in MCT1 in the endothelial cells lining the blood–brain barrier.<sup>37</sup> Similarly, we observed increased immunoreactivity for MCT1 in a KD-fed rat glioma, indicating a KD-induced adaptation that facilitates uptake of blood-borne BHB. Recently De Saedeleer et al.<sup>38</sup> showed

in human cervix cancer cells that glucose lowering in growth media dose-dependently ( $<1$  mM) upregulated MCT1 and CD147 expression. CD147 (basigin) is the chaperone protein required for functioning of MCT1.<sup>39</sup> Because the KD used in the present study led to lower plasma glucose concentrations compared with the standard diet (Fig. 4A), it is possible that the glioma cells upregulated the activity of MCT1 and/or CD147 in a similar glucose level-dependent manner as reported by De Saedeleer et al.<sup>38</sup>

Studies on the KD as anticancer therapy vary in diet composition, start of the diet, and calorie restriction. To accomplish significant lowering of plasma glucose in rodents, a KD needs to be combined with calorie restriction. This complicates identifying whether reduced glucose or calorie restriction in general is dominant when observing a therapeutic effect. Despite establishing low glucose and high BHB levels in plasma—at the cost of some body weight loss—our KD did not result in a slowing down of tumor growth or increase in survival in either glioma model. These results are not in line with the successful growth-inhibiting effect reported in mouse astrocytomas and gliomas.<sup>6,8,10,20,25,32</sup> Potentially the cancer cell lines used in the mouse models did lack ketolytic activity, in contrast to RG2 and 9L gliomas *in vivo*. Another possible explanation is the timing of the KD: we started the diet one week after implantation for tumor cells to grow because this resembles more closely the scenario that patients would encounter. Previous studies have started animals on the KD closer to the time of tumor cell implantation.<sup>4,6,8,10,25,32</sup> However, the lack of tumor growth inhibition is not a completely unique observation. Dang et al.<sup>40</sup> did not see an effect in a mouse model of hedgehog pathway medulloblastoma. Similarly, Woolf et al.<sup>41</sup> while reporting KD-induced effects on several proteins involved in malignant progression, observed no tumor growth inhibition. We currently cannot identify whether differences in the application of KDs, differences in tumor models, or other unknown factors are the culprit of the varying results.

A limitation of the present study is the inclusion of rat glioma models only. Following the unanticipated observation that a KD did not inhibit tumor growth and had no effect on survival, inclusion of mouse models in which KDs are successful as anticancer therapy is warranted. However, given that we did not see an inhibiting effect on tumor growth or animal survival when fed a KD, one could argue that our data do not dismiss the proposed mechanism: lack of ketolytic activity could be a requirement for a KD to be successful in slowing down tumor growth. More studies are needed to resolve the relation between tumor growth inhibition and diet-induced ketosis in other *in vivo* tumor models, and particularly in patients. The noninvasive character of MRS could be exploited to evaluate the degree of BHB oxidation in patients' gliomas analogously to the present study. If the capacity to oxidize BHB in gliomas varies with tumor type and/or molecular background, presence or absence of glioma ketolysis could be a selection criterion for clinical trials investigating the KD, as suggested by Chang et al.<sup>27</sup> However, the question remains whether adaptations occur in tumors that initially show apparent low ketolytic enzyme activity to increase ketone body metabolism when exposed to a KD, analogous to the increased MCT1 expression observed in this study. An example of potential KD-induced changes in brain could come from observations in a subset of

type I diabetes subjects. Hypoglycemia-unaware type I diabetes patients have been shown to have increased transport capacity in the blood–brain barrier for monocarboxylic acids (primarily acetate, lactate, BHB, acetoacetate).<sup>42</sup> Type I diabetes patients become “hypoglycemia unaware” when they experience recurrent periods of low plasma glucose levels, and the increased transport capacity is believed to involve the MCT1/CD147 complex.<sup>43</sup> Similar to the mechanism discussed by De Saedeleer et al and the observation in hypoglycemia-unaware patients, KD-induced low plasma glucose levels could stimulate the MCT1/CD147 complex and thereby facilitate ketone body oxidation in both normal and neoplastic brain tissue in humans.<sup>38,44</sup>

Other potential effects of a KD, yet beyond the scope of this paper, are the role of BHB as an inhibitor of class I histone deacetylases and the neuroprotective role of BHB through binding to the hydroxy-carboxylic acid receptor 2 (HCA2, GPR109A) on monocytes and macrophages.<sup>45,46</sup> We did not investigate the presence of such nonmetabolic effects of BHB in our glioma models, as tumor growth was not obviously affected.

In conclusion, our *in vivo* data showed that there was no difference in the relative levels of ketone body oxidation between gliomas and normal brain tissue. Based on the present data, the main proposed rationale to use a KD as brain tumor therapy—the lack of ketolytic activity in brain tumors<sup>4–12</sup>—does not apply to our rat glioma models. Additionally, the KD can stimulate ketone body uptake in gliomas, presumably via an increase in MCT1, thereby facilitating ketone body oxidation. These results indicate that brain tumors can have a high degree of metabolic flexibility that needs to be taken into account in the design of metabolism-targeted therapies. Future studies should take advantage of the noninvasive character of <sup>13</sup>C MRS and study brain tumor metabolism *in vivo* to reveal the level of ketone body oxidation in human brain tumors.

Additional information and data are available in the Supplementary material.

## Supplementary material

Supplementary material is available online at *Neuro-Oncology* (<http://neuro-oncology.oxfordjournals.org/>).

## Funding

H. M.D.F. was supported by fellowship 10A087 from the American Institute for Cancer Research and a 2013 Discovery Award from the American Brain Tumor Association. F.H. was supported by NIH grants P30-NS052519, R01 EB-011968, and R01 CA-140102. As members of the Yale Cancer Center, H.M.D.F. and F.H. are supported by NIH grant CA-16359 from the National Cancer Institute.

## Acknowledgments

We acknowledge help from Drs Eric Shapiro, Maggie Bennewitz, Christoph Juchem, Xenophon Papademetris, Susan Mayne, Robert Dubrow, Daniel Coman, Yuegao Huang, and Jon Arellano. We thank Bei Wang and Shauna Quinn for assistance with animal preparation; and Terry Nixon, Scott McIntyre, and Peter Brown for maintenance and upgrades to the MR system.

*Conflict of interest statement.* The authors have no conflicts of interest to disclose.

## References

- Pan JW, de Graaf RA, Petersen KF, et al. [2,4-13C2]- $\beta$ -Hydroxybutyrate metabolism in human brain. *J Cereb Blood Flow Metab.* 2002;22(7):890–898.
- Owen OE, Morgan AP, Kemp HG, et al. Brain metabolism during fasting\*. *J Clin Invest.* 1967;46(10):1589–1595.
- Skinner R, Trujillo A, Ma X, et al. Ketone bodies inhibit the viability of human neuroblastoma cells. *J Pediatr Surg.* 2009;44(1):212–216.
- Seyfried TN, Sanderson TM, El-Abbadi MM, et al. Role of glucose and ketone bodies in the metabolic control of experimental brain cancer. *Br J Cancer.* 2003;89(7):1375–1382.
- Seyfried TN, Mukherjee P. Targeting energy metabolism in brain cancer: review and hypothesis. *Nutr Metab.* 2005;2(1):30.
- Zhou W, Mukherjee P, Kiebish MA, et al. The calorically restricted ketogenic diet, an effective alternative therapy for malignant brain cancer. *Nutr Metab.* 2007;4:5.
- Seyfried TN, Flores R, Poff AM, et al. Metabolic therapy: a new paradigm for managing malignant brain cancer. *Cancer Lett.* 2015;356(2, Part A):289–300.
- Mukherjee P, El-Abbadi MM, Kasperzyk JL, et al. Dietary restriction reduces angiogenesis and growth in an orthotopic mouse brain tumour model. *Br J Cancer.* 2002;86(10):1615–1621.
- Klement RJ, Kämmerer U. Is there a role for carbohydrate restriction in the treatment and prevention of cancer? *Nutr Metab.* 2011;8:75.
- Marsh J, Mukherjee P, Seyfried TN. Drug/diet synergy for managing malignant astrocytoma in mice: 2-deoxy-D-glucose and the restricted ketogenic diet. *Nutr Metab.* 2008;5:33.
- Tisdale MJ, Brennan RA. Loss of acetoacetate coenzyme A transferase activity in tumours of peripheral tissues. *Br J Cancer.* 1983;47(2):293–297.
- Woolf EC, Scheck AC. The ketogenic diet for the treatment of malignant glioma. *J Lipid Res.* 2015;56(1):5–10.
- Schmidt M, Pfetzer N, Schwab M, et al. Effects of a ketogenic diet on the quality of life in 16 patients with advanced cancer: A pilot trial. *Nutr Metab.* 2011;8:54.
- Champ CE, Palmer JD, Volek JS, et al. Targeting metabolism with a ketogenic diet during the treatment of glioblastoma multiforme. *J Neurooncol.* 2014;117(1):125–131.
- Rieger J, Bähr O, Maurer GD, et al. ERGO: A pilot study of ketogenic diet in recurrent glioblastoma. *Int J Oncol.* 2014;44(6):1843–1852.
- Nebeling LC, Miraldi F, Shurin SB, et al. Effects of a ketogenic diet on tumor metabolism and nutritional status in pediatric oncology patients: two case reports. *J Am Coll Nutr.* 1995;14(2):202–208.
- Zuccoli G, Marcello N, Pisanello A, et al. Metabolic management of glioblastoma multiforme using standard therapy together with a restricted ketogenic diet: case report. *Nutr Metab.* 2010;7:33.
- Schwartz K, Chang HT, Nikolai M, et al. Treatment of glioma patients with ketogenic diets: report of two cases treated with an IRB-approved energy-restricted ketogenic diet protocol and review of the literature. *Cancer Metab.* 2015;3(1):3.
- Allen BG, Bhatia SK, Buatti JM, et al. Ketogenic diets enhance oxidative stress and radio-chemo-therapy responses in lung



- cancer xenografts. *Clin Cancer Res Off J Am Assoc Cancer Res.* 2013;19(14):3905–3913.
20. Poff AM, Ari C, Seyfried TN, et al. The ketogenic diet and hyperbaric oxygen therapy prolong survival in mice with systemic metastatic cancer. *PLoS One.* 2013;8(6):e65522.
  21. Poff A, Ari C, Arnold P, et al. Ketone supplementation decreases tumor cell viability and prolongs survival of mice with metastatic cancer. *Int J Cancer J Int Cancer.* 2014;135(7):1711–1720.
  22. Caso J, Masko EM, Thomas JA, et al. The effect of carbohydrate restriction on prostate cancer tumor growth in a castrate mouse xenograft model. *The Prostate.* 2013;73(5):449–454.
  23. Ho VW, Leung K, Hsu A, et al. A low carbohydrate, high protein diet slows tumor growth and prevents cancer initiation. *Cancer Res.* 2011;71(13):4484–4493.
  24. Ho VW, Hamilton MJ, Dang N-HT, et al. A low carbohydrate, high protein diet combined with celecoxib markedly reduces metastasis. *Carcinogenesis.* 2014;35(10):2291–2299.
  25. Abdelwahab MG, Fenton KE, Preul MC, et al. The ketogenic diet is an effective adjuvant to radiation therapy for the treatment of malignant glioma. *PLoS One.* 2012;7(5).
  26. Maurer GD, Brucker DP, Bähr O, et al. Differential utilization of ketone bodies by neurons and glioma cell lines: a rationale for ketogenic diet as experimental glioma therapy. *BMC Cancer.* 2011;11:315.
  27. Chang HT, Olson LK, Schwartz KA. Ketolytic and glycolytic enzymatic expression profiles in malignant gliomas: implication for ketogenic diet therapy. *Nutr Metab.* 2013;10:47.
  28. Marin-Valencia I, Yang C, Mashimo T, et al. Analysis of tumor metabolism reveals mitochondrial glucose oxidation in genetically diverse human glioblastomas in the mouse brain in vivo. *Cell Metab.* 2012;15(6):827–837.
  29. Mashimo T, Pichumani K, Vemireddy V, et al. Acetate is a bioenergetic substrate for human glioblastoma and brain metastases. *Cell.* 2014;159(7):1603–1614.
  30. de Graaf RA, Rothman DL, Behar KL. State of the art direct 13C and indirect 1H-[13C] NMR spectroscopy in vivo. A practical guide. *NMR Biomed.* 2011;24(8):958–972.
  31. Barth RF, Kaur B. Rat brain tumor models in experimental neuro-oncology: the C6, 9L, T9, RG2, F98, BT4C, RT-2 and CNS-1 gliomas. *J Neurooncol.* 2009;94(3):299–312.
  32. Stafford P, Abdelwahab MG, Kim DY, et al. The ketogenic diet reverses gene expression patterns and reduces reactive oxygen species levels when used as an adjuvant therapy for glioma. *Nutr Metab.* 2010;7:74.
  33. De Graaf RA, Chowdhury GMI, Brown PB, et al. In situ 3D magnetic resonance metabolic imaging of microwave-irradiated rodent brain: a new tool for metabolomics research. *J Neurochem.* 2009;109(2):494–501.
  34. Berkel A, van Rao JU, Kusters B, et al. Correlation between in vivo 18F-FDG PET and immunohistochemical markers of glucose uptake and metabolism in pheochromocytoma and paraganglioma. *J Nucl Med.* 2014;55(8):1253–1259.
  35. Eloqayli H, Melø TM, Hauvik A, et al. [2,4-13C]β-hydroxybutyrate metabolism in astrocytes and C6 glioblastoma cells. *Neurochem Res.* 2011;36(8):1566–1573.
  36. Halestrap AP, Wilson MC. The monocarboxylate transporter family—role and regulation. *IUBMB Life.* 2012;64(2):109–119.
  37. Leino RL, Gerhart DZ, Duelli R, et al. Diet-induced ketosis increases monocarboxylate transporter (MCT1) levels in rat brain. *Neurochem Int.* 2001;38(6):519–527.
  38. De Saedeleer CJ, Porporato PE, Copetti T, et al. Glucose deprivation increases monocarboxylate transporter 1 (MCT1) expression and MCT1-dependent tumor cell migration. *Oncogene.* 2014;33(31):4060–4068.
  39. Halestrap AP. The monocarboxylate transporter family—structure and functional characterization. *IUBMB Life.* 2012; 64(1):1–9.
  40. Dang MT, Wehrli S, Dang CV, et al. The ketogenic diet does not affect growth of hedgehog pathway medulloblastoma in mice. *PLoS One.* 2015;10(7):e0133633.
  41. Woolf EC, Curley KL, Liu Q, et al. The ketogenic diet alters the hypoxic response and affects expression of proteins associated with angiogenesis, invasive potential and vascular permeability in a mouse glioma model. *PLoS One.* 2015;10(6):e0130357.
  42. De Feyter HM, Mason GF, Shulman GI, et al. Increased brain lactate concentrations without increased lactate oxidation during hypoglycemia in type 1 diabetic individuals. *Diabetes.* 2013; 62(9):3075–3080.
  43. Cryer PE. Mechanisms of hypoglycemia-associated autonomic failure in diabetes. *N Engl J Med.* 2013;369(4):362–372.
  44. Froberg MK, Gerhart DZ, Enerson BE, et al. Expression of monocarboxylate transporter MCT1 in normal and neoplastic human CNS tissues. *Neuroreport.* 2001;12(4):761–765.
  45. Shimazu T, Hirschey MD, Newman J, et al. Suppression of oxidative stress by β-hydroxybutyrate, an endogenous histone deacetylase inhibitor. *Science.* 2013;339(6116):211–214.
  46. Rahman M, Muhammad S, Khan MA, et al. The β-hydroxybutyrate receptor HCA2 activates a neuroprotective subset of macrophages. *Nat Commun.* 2014;5:3944.